DOI 10.4430/bgta0294

Magma storage and ascent during the largest eruption of Somma-Vesuvius volcano: Pomici di Base (22 ka) Plinian event

G. Buono[1,2], L. Pappalardo[1] and P. Petrosino[2]

[1] *Istituto Nazionale di Geofisica e Vulcanologia, Osservatorio Vesuviano, Napoli, Italy*
[2] *Dipartimento di Scienze della Terra, dell'Ambiente e delle Risorse, Università degli Studi Federico II, Napoli, Italy*

(Received: 26 March 2019; accepted: 16 July 2019)

ABSTRACT The reconstruction of the pre-eruptive storage conditions as well as syn-eruptive magma ascent dynamics of past eruptions is of fundamental importance to decipher the relationship between surface-monitored signals and the sub-volcanic processes in order to learn more about the eruptive behaviour of active volcanoes. The Pomici di Base Plinian eruption is the first (22 ka) and largest (> 4.4 km^3) event of the Somma-Vesuvius volcanic complex. Here we present the preliminary results of a geochemical, isotopic, two-dimensional and three-dimensional textural study performed on volcanic products emitted during the Plinian phase of this eruptive event with the aim to reconstruct in more details the magmatic evolution of this large caldera-forming eruption. Particularly, it was fed by chemically and thermally zoned magmas extracted from a crystal mush zone in a magma chamber with top at ~4.5 km depth. During this eruption, crustal (limestone) contamination and subsequent CO_2 emissions as well as changes in degassing mechanisms mainly controlled the eruptive dynamics.

Key words: Somma-Vesuvius, Plinian eruptions, magma storage and ascent.

1. Introduction

The knowledge of processes occurred in magma chamber and volcanic conduit during high-magnitude eruptions is a primary goal in volcanology, due to the influence of these sub-volcanic processes on the behaviour of precursory phenomena that are detected by monitoring systems during volcanic crises. In fact, a severe difficulty in volcanic forecast is to correlate the evolution of the geochemical and geophysical signals recorded at the surface with the dynamics of magma transfer at depth. In details, magma migration towards the surface is strongly controlled by intensive magmatic variables (e.g. magma and volatiles composition, temperature) as well as storage (e.g. depth and volume of magma chambers) and ascent (e.g. decompression rate, open vs. closed degassing regime) conditions (e.g. Gonnermann and Manga, 2007; Blundy and Cahsman, 2008), which can be influenced by external factors [e.g. edifice load and related stress field, conduit geometry, interaction with country rocks or external water; e.g. Borgia *et al*. (2005) and Houghton *et al*. (2010)].

In the last decades, quantitative textural studies on volcanic rocks combined with conventional geochemical analyses, have proved to be a fundamental approach in exploring the pre-eruptive

© 2020 – OGS

and syn-eruptive conditions allowing us to improve our ability to interpret volcano-monitoring signals and perform hazard assessments. In particular, the 3D textural investigation in the last two decades has been successfully applied in several field of geosciences (e.g. Cnudde and Boone, 2013) and recently many studies have demonstrated the potential of this technique also to examine volcanic processes (e.g. Shea *et al.*, 2010; Baker *et al.*, 2012).

In more densely populated regions, as the Neapolitan high-risk volcanic area, this information would be essential for a better assessment of the volcanic hazard.

In this case study we have performed a geochemical (major-minor elements and Sr-Nd isotopic ratios) and 2D and 3D textural investigation of volcanic products emitted during the Pomici di Base Plinian eruption of Somma-Vesuvius volcano. This event represents the first (22 ka) and largest (volume larger than 4.4 km^3) explosive eruption of Somma-Vesuvius volcano (Bertagnini *et al.*, 1998; Landi *et al.*, 1999). Moreover, it delineates the end of a period of open-conduit activity and the transition to the explosive character of the volcano as well as the beginning of caldera collapse events (e.g. Cioni *et al.*, 2008; Santacroce *et al.*, 2008; De Vivo *et al.*, 2010). The obtained preliminary results allowed us to achieve information on the evolution of plumbing system and eruptive dynamics during this eruption.

2. Volcanological background

The Somma-Vesuvius volcano, located at the SE of metropolitan area of Naples, is one of the most dangerous volcanoes in the world (Fig. 1a). The strato-volcano consists of the old edifice of Mt. Somma, featured by a summit caldera structure occupied in its centre by the younger Vesuvius cone, whose last eruption occurred in 1944 (e.g. Cole and Scarpati, 2010; Pappalardo *et al.*, 2014; Cubellis *et al.*, 2016). The volcanism started with an early period of effusive and slightly explosive activity of the Mt. Somma, interrupted more than 22 ka and followed by a period characterised by at least four Plinian eruptions (Pomici di Base, Mercato Pumice, Avellino Pumice, Pompeii Pumice; Fig. 1b) staggered with minor events covering a large range of magnitude and intensity. After 79 A.D. (Pompeii Pumice) eruption, the Vesuvius cone began to form during periods of open conduit activity, the last of which manifested in 1631-1944, ended with the current quiescent state (e.g. Cioni *et al.*, 2008; Santacroce *et al.*, 2008; De Vivo *et al.*, 2010).

The Somma-Vesuvius volcanic products can be subdivided into three potassic and high-potassic series on the basis of their chemical compositions (Fig. 1c): 1) slightly silica-undersaturated series, older than 9 ka; 2) mildly silica-undersaturated series, between 9 and 2 ka; 3) strongly silica-undersaturated series, younger than 2 ka (Joron *et al.*, 1987). The large variability of Somma-Vesuvius magmas has been related to changes in the primary melts feeding the activity and to the effect of shallow level crystallisation under different thermodynamic conditions (e.g. Santacroce, 1987; Civetta *et al.*, 1991; Belkin and De Vivo, 1993; Santacroce *et al.*, 1993; Trigila and De Benedetti, 1993; Marianelli *et al.*, 1995, 1999, 2005; Ayuso *et al.*, 1998; Cioni *et al.*, 1998; Cioni, 2000; Lima *et al.*, 2003; Peccerillo, 2005; Mastrolorenzo and Pappalardo, 2006; Di Renzo *et al.*, 2007; Scandone *et al.*, 2007; Scaillet *et al.*, 2008; Pappalardo and Mastrolorenzo, 2010, 2012). Moreover, several geochemical studies have stressed the importance of crustal contamination in the evolution of Vesuvius magma (e.g. Savelli, 1968; Fulignati *et al.*, 1995, 1998; Gilg *et al.*, 1999, 2001; Del Moro *et al.*, 2001; Pappalardo *et al.*,

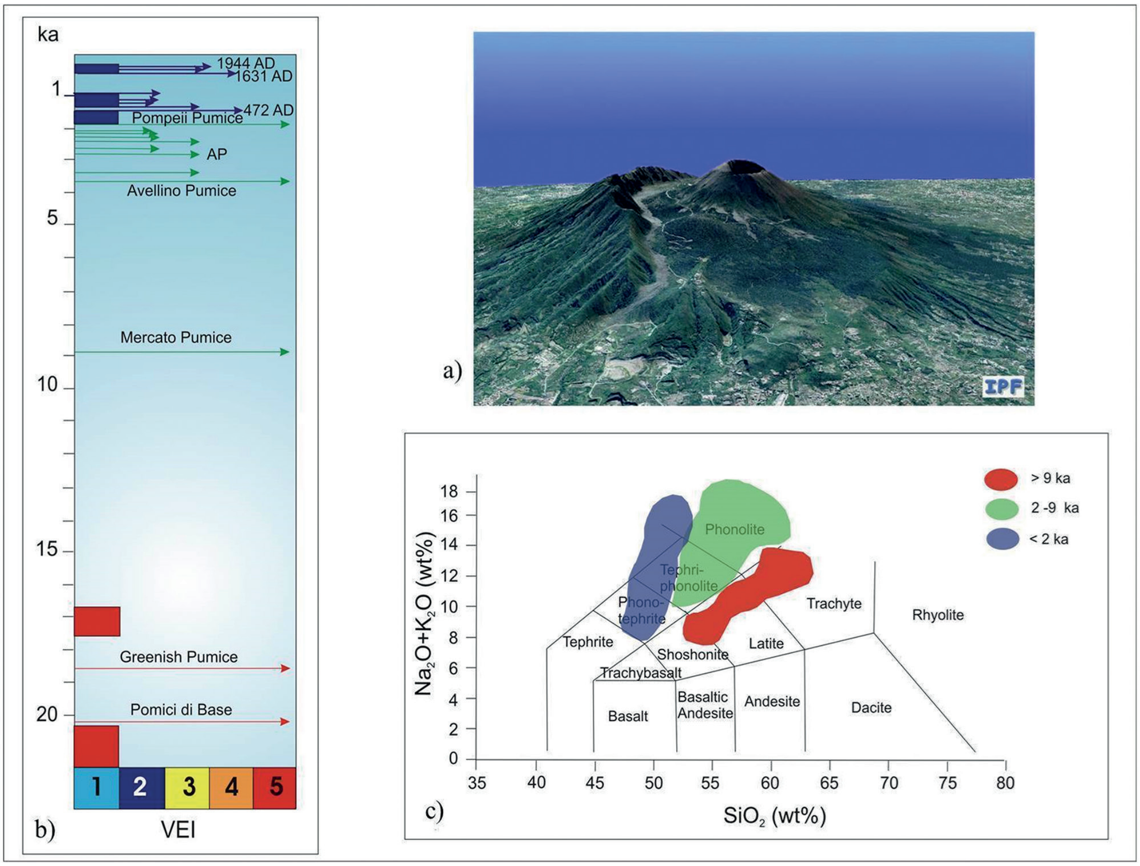

Fig. 1 - a) 3D view of current Somma-Vesuvius volcano (courtesy of G. Vilardo); b) schematic chronogram of Somma-Vesuvius activity as recorded by stratigraphic successions (after Cioni *et al.*, 2008); c) Total Alkalis vs. Silica (TAS) for Somma-Vesuvius rocks (after Santacroce *et al.*, 2008). Colours are related to volcanism older than 9 ka (red), between 9 and 2 ka (green) and younger than 2 ka (blue).

2004; Piochi *et al.*, 2006; Iacono Marziano *et al.,* 2008, 2009; Dallai *et al.*, 2011; Jolis *et al.*, 2013, 2015; Pichavant *et al.*, 2014).

Degassing during Somma-Vesuvius eruptions was investigated in several textural studies (Mastrolorenzo and Pappalardo, 2006; Pappalardo and Mastrolorenzo, 2010; Cioni *et al.*, 2011; Shea *et al.*, 2012; Pappalardo *et al.*, 2014; Zdanowicz *et al.*, 2018). Closed-system degassing regime during fast magma ascent (from hours to days) and open-system degassing regime during slow magma ascent (from days to months) have been invoked for highly explosive and moderately explosive-effusive events respectively, resulting in a general decrease in bulk vesicularity and increase in degassing-induced microlites content in juvenile products as the volcanic explosive index (VEI) decrease (e.g. Mastrolorenzo and Pappalardo, 2006; Pappalardo and Mastrolorenzo, 2010).

The Plinian Pomici di Base eruption is the oldest and largest explosive event generated by the Somma-Vesuvius volcano (e.g. Delibrias *et al.*, 1979; Bertagnini *et al.*, 1998; Landi *et al.*, 1999). The eruption occurred from a vent located 1.0-2.5 km west of the present cone, the eruptive column reached a height of 15-17 km (mass discharge rate, MDR = 2.0-2.5×10^7 kg/s) and emplaced a volcanic deposit with volume higher than 4.4 km^3 (Bertagnini *et al.*, 1998).

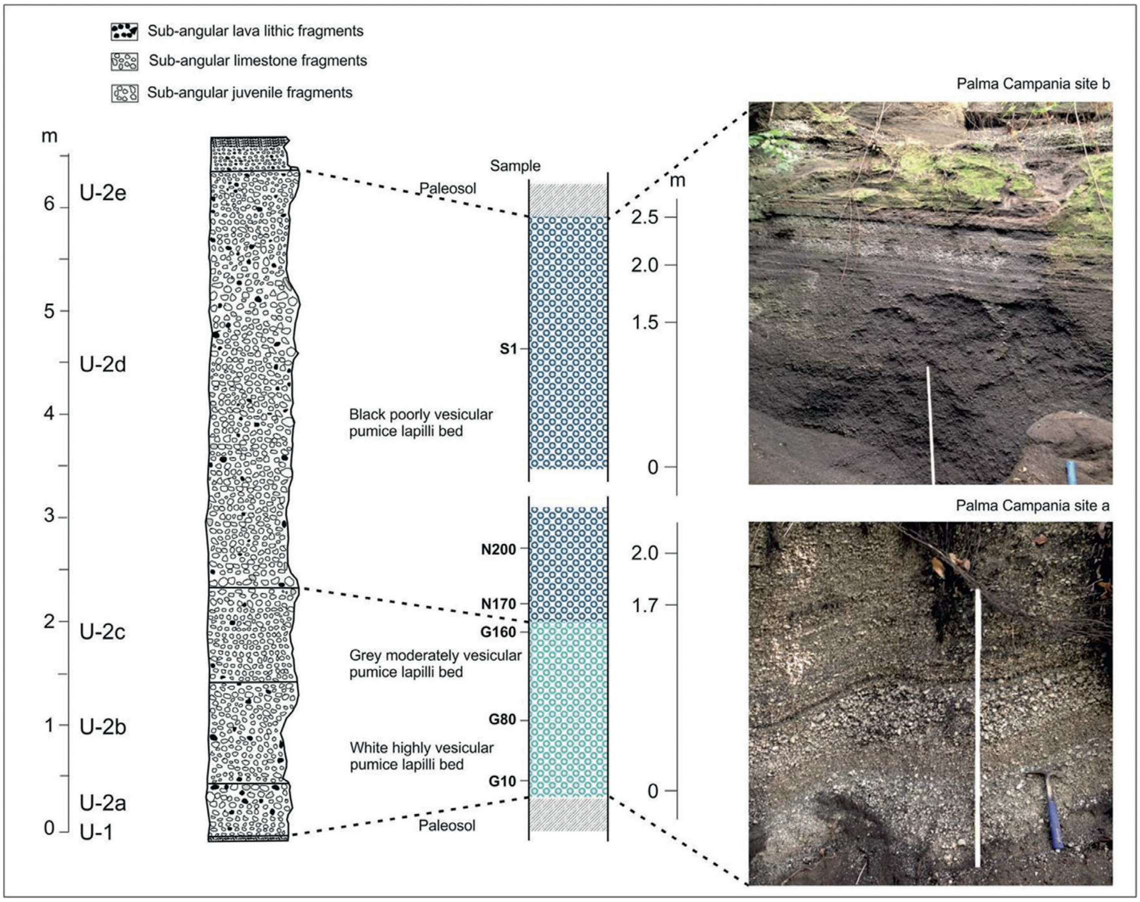

Fig. 2 - Representative photos and schematic stratigraphic column for the Pomici di Base eruption and localisation of samples collected for this study. The sampling interval (on the left) was dictated by changes in grain size and colour, according to the different stratigraphic units recognised by Bertagnini *et al.* (1998).

Delibrias *et al.* (1979) were the first to recognise the Plinian character of this event and obtained a ^{14}C age of 17050±140 yr B.P. on the paleosol underneath the deposits, in agreement with the values of 18750±420 - 19170±420 yr B.P. measured by Bertagnini *et al.* (1998). Other studies measured an age of about 22 ka by using K/Ar method on sanidine [22520±1000 yr B.P.: Capaldi *et al.* (1985)] and ^{14}C method on charcoal [maximum cal. age of 22030±175 yr B.P.: Andronico *et al.* (1995) and Siani *et al.* (2004)].

Bertagnini *et al.* (1998) recognised three different eruptive phases: 1) an early opening phase, during which thin ash and pumice fall deposits were emplaced (U-1 in Fig. 2); 2) a Plinian phase, principally consisting of a fallout deposit (U-2 in Fig. 2), although on the volcano's slopes small-volume pyroclastic density currents (PDCs; pyroclastic surge) units are recognisable. The Plinian fallout is composed by three different layers: a basal white pumiceous layer (U-2a and U-2b), a transitional layer (U-2c), an upper thick black scoria bed (U-2d and U-2e), with a relative thickness of 2:1:5; 3) a final phreatomagmatic phase, during which a lithic-rich fallout and PDCs (pyroclastic surge and flow) deposits [U-3/U-6 in Bertagnini *et al.* (1998)] were generated, associated with caldera collapse (Bertagnini *et al.*, 1998; Cioni *et al.*, 1999).

Magma storage zone as well as syn-eruptive dynamics are debated. Landi *et al*. (1999) proposed that the eruption was fed by a low-aspect-ratio trachytic-latitic magma chamber located at pressure of about 300-400 MPa and hypothesised the replenishment of shoshonitic magma as eruption trigger. On the contrary, Balcone-Boissard *et al*. (2015) obtained a shallower pressure value of 100 MPa for the magmatic reservoir of the Pomici di Base eruption deduced from the Cl-buffering effect. Recently Pappalardo *et al*. (2018) proposed that limestone contamination could have been a significant process affecting both magma evolution as well as eruptive dynamics.

3. Methods

3.1. Density analysis

In order to account for possible density variations with size, we used clasts within a -5 to -2 phi size range for density measurements. Sets of 100 clasts for each granulometric class (where present) were weighted and coated with a thin film of paraffin wax, then their density was determined using a water pycnometer. We considered the volume of the paraffin wax film to be negligible because its density was about equal to that of water (1 g/cm^3). We obtained bulk vesicularities by comparing the densities of juvenile vesicular clasts with the dense-rock equivalent densities (2.4 and 2.6 g/cm^3 for pumices and scoriae respectively) for the composition of interest [as in Houghton and Wilson (1989)]. Modal density/vesicularity clasts were selected for textural and geochemical analysis (see Balcone-Boissard *et al*., 2015 and reference therein).

3.2. Geochemical analyses

Major-minor elements and Cl contents of matrix-glass and minerals (feldspars and pyroxenes) compositions were measured by scanning electron microscope (SEM) JEOL JSM 5310 (15 kV, ZAF Correction Routine) with energy dispersive spectrometer (EDS) at CISAG (Centro Interdipartimentale di Servizio per Analisi Geomineralogiche) at the University of Naples Federico II. Instrument calibration was based on international mineral and glass standards. Mean precision was less than 5% for SiO_2, Al_2O_3, K_2O, CaO, FeO and around 10% for the other elements (e.g. Morabito *et al*., 2014).

3.3. Radiogenic isotopes

Isotopic analyses for Sr and Nd via thermal ionisation mass spectrometry (TIMS) were obtained at the Istituto Nazionale di Geofisica e Vulcanologia - Sezione di Napoli ''Osservatorio Vesuviano'' (INGV-OV), using a ThermoFinnigan Triton TI multi-collector mass spectrometer. Samples were processed through conventional HF-HNO_3-HCl dissolution before Sr and middle REE (MREE) were separated by standard cation exchange column chemistry, and Nd was further purified on an anion column. Sr and Nd were then loaded onto Ta and Re filaments, respectively. Sr and Nd blanks were negligible for the analysed samples during the periods of measurements. Measured $^{87}Sr/^{86}Sr$ ratios were normalised for within-run isotopic fractionation to $^{87}Sr/^{86}Sr$ = 0.1194, and $^{143}Nd/^{144}Nd$ ratios to $^{143}Nd/^{144}Nd$ = 0.7219. The mean measured value of $^{87}Sr/^{86}Sr$ for NIST-SRM 987 was 0.710215±0.000008 (2σ, n = 36) and of $^{143}Nd/^{144}Nd$ for La Jolla was 0.511843±0.000006 (2σ, n = 11). The quoted error is the standard deviation of the mean (2σ) for n = 180. Sr and Nd isotope ratios have been normalised to the recommended values of NIST SRM 987 ($^{87}Sr/^{86}Sr$ = 0.71025) and La Jolla ($^{143}Nd/^{144}Nd$ = 0.51185) standards, respectively.

3.4. Textural analyses

The microstructure of the sample was investigated by X-ray microtomography (μCT) using a Carl Zeiss Xradia 410 Versa 3D X-ray microscope at the INGV-OV, selecting representative pumice and scoria clasts less than 3-4 cm in diameter, that cooled rapidly, thus reducing post-fragmentation vesicle expansion effects (e.g. Thomas and Sparks, 1992; Tait *et al*., 1998). In detail, μCT allowed us the direct observation and 3D quantitative characterisation of the number and size of vesicles, which are impossible to determine using conventional 2D techniques and constitute fundamental parameters to investigate magma degassing during its ascent towards the surface.

μCT images were acquired on each sample at different optical magnification (10X and 20X). Cylinders of 0.5 cm in diameter were cut from the representative samples and the scan was performed over a 360° rotation using 4001 projections, 80 KV voltage, 10 W power. The resulting nominal voxel (volumetric pixel) size ranges from 0.9 to 2.0 μm depending on the magnification used. Reconstruction of the attenuation data was performed using filtered back-projection, producing a stack of 967 cross-sectional, grey-scale digital images. Vesicles forming the pore network have been analysed by segmenting and processing regions of a given range of grayscale values from the rest of the image using the Avizo software.

Finally, microlite content was measured acquiring for each sample at least 4-5 back-scattered electron (BSE) 2D images (270×200 μm) with SEM, then processed and analysed using ImageJ software.

4. Results

4.1. Petrographic features

Qualitative preliminary observations of thin sections under polarising microscope and 2D/3D images reveal that the collected samples from the base to the top of fallout units have porphyritic texture with low content of phenocrysts (< 5 vol.%) that are present as isolated crystals as well as in aggregate. Crystals have a maximum size of 3 mm and are constituted in order of decreasing abundance by sanidine>plagioclase>clinopyroxene>biotite and in minor amount by amphibole, magnetite and garnet. The content of plagioclase and mafic minerals increases in scoria samples at the top of the stratigraphic sequence, in which they appear also as discrete micro-phenocrysts (<< 1 mm). Generally, phenocrysts show euhedral or sub-euhedral habit, however minor evidence of disequilibrium is observed (e.g. irregular edges, zoned clinopyroxene crystals with a marked "resorbed core").

The degree of vesicularity and crystallisation (microlite) varies progressively in the matrix glass from the bottom upwards in the stratigraphic sequence. In particular, the basal and intermediate (white to gray) pumice samples show high vesicularity and absence of microlites, while the upper black scoria are characterised by poorly-vesiculated, microlite-rich groundmass (Fig. 3).

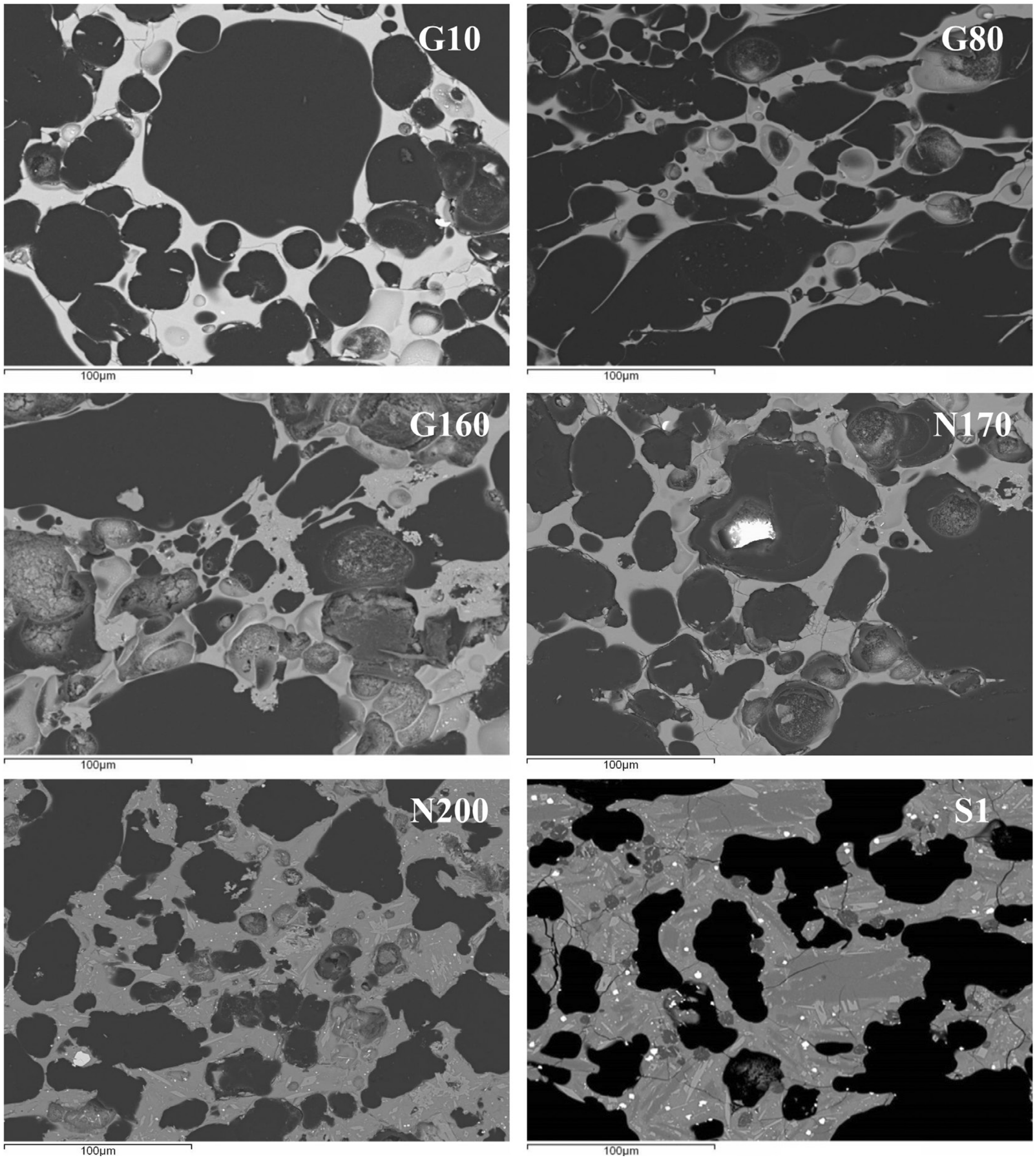

Fig. 3 - Representative back-scattered electron images of juvenile rocks from Pomici di Base eruption.

4.2. Glass composition

In the classification Total Alkali versus Silica diagram (TAS, Fig. 1), the composition of the analysed matrix-glasses ranges from trachyte (white to gray pumices) to latite (black scoriae) upwards of stratigraphic succession.

On Harker variation diagrams (Fig. 4), there is a systematic increase in SiO_2 and Na_2O as well as a regular decrease in TiO_2, FeO, CaO, P_2O_5 and Cl with the decrement of MgO content, chosen as differentiation index. The concentrations of Al_2O_3 and MnO remain roughly constant, while K_2O content weakly increases in the less evolved rocks and then remains constant in the course of differentiation (Fig. 4 and Table 1).

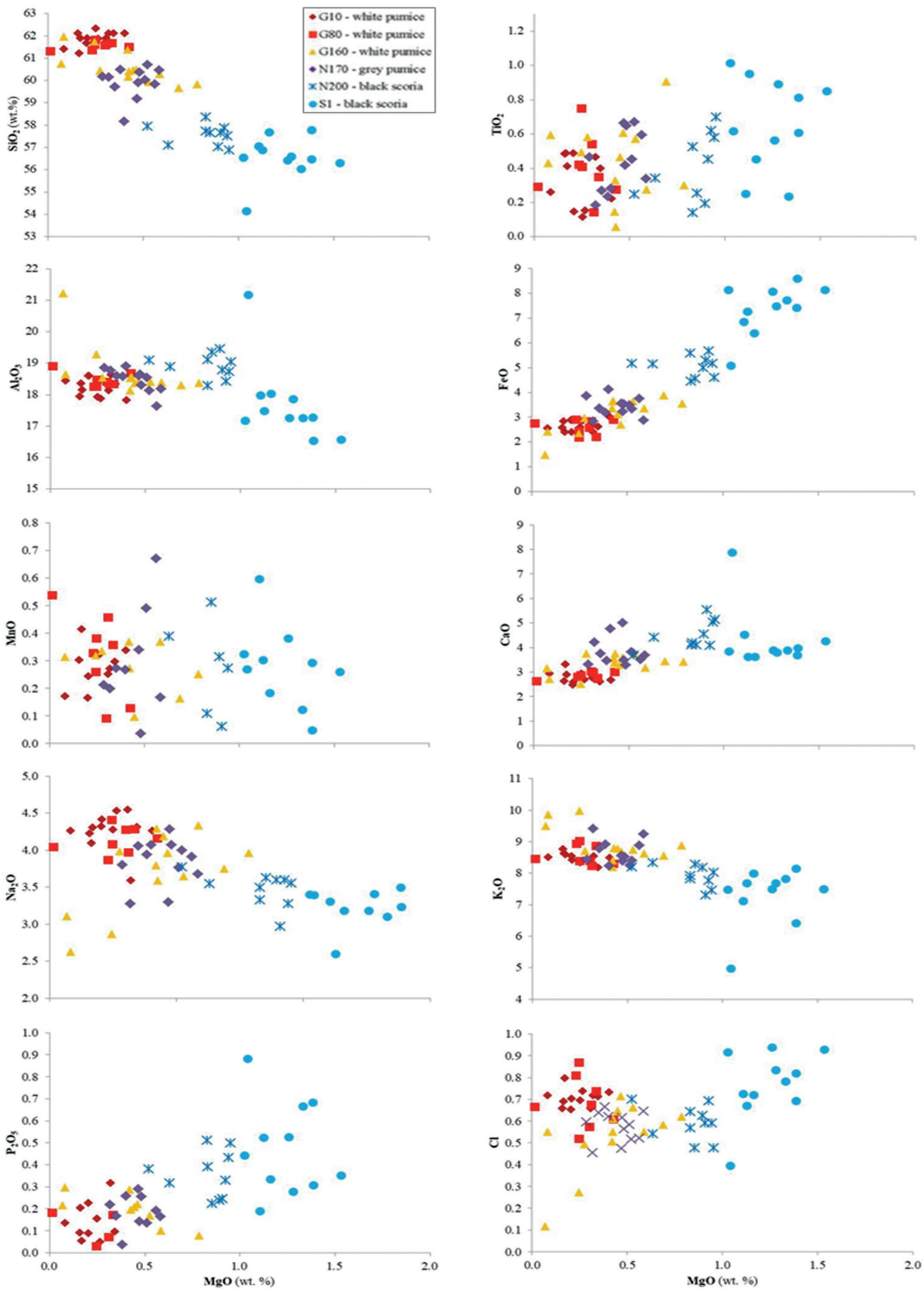

Fig. 4 - Major element variation diagrams for Pomici di Base rocks.

Table 1 - Geochemical composition of representative glasses and phenocrysts (data refer to microlites only for sample S1) in the analysed samples. Value in brackets is 2σ (standard deviation). pl=plagioclase, sn=sanidine, cpx=clinopyroxene.

Sample	**G10**				**G80**				**G160**			
phase	*glass*	*pl*	*sn*	*cpx*	*glass*	*pl*	*sn*	*cpx*	*glass*	*pl*	*sn*	*cpx*
# of analyses	12	5	1	2	8	1	0	1	13	4	0	1
SiO_2	60.13 (1.91)	52.74 (4.54)	64.87	48.02 (0.50)	60.30 (1.35)	52.40		44.39	59.73 (2.14)	50.50 (3.55)		47.45
TiO_2	0.29 (0.33)	0.12 (0.38)	0.00	0.70 (0.37)	0.39 (0.36)	0.13		2.16	0.44 (0.44)	0.06 (0.14)		1.02
Al_2O_3	17.70 (0.71)	30.18 (4.23)	19.53	4.26 (2.39)	18.06 (0.62)	29.50		8.58	18.43 (1.62)	31.25 (1.58)		5.52
FeO	2.56 (0.44)	0.44 (0.25)	0.15	12.73 (1.87)	2.53 (0.58)	0.77		13.07	3.02 (1.35)	0.61 (0.61)		13.26
MnO	0.23 (0.25)	0.00 (0.00)	0.07	0.57 (0.23)	0.31 (0.30)	0.16		0.22	0.19 (0.30)	0.07 (0.26)		0.50
MgO	0.24 (0.18)	0.06 (0.13)	0.03	9.70 (0.24)	0.26 (0.23)	0.00		9.02	0.42 (0.43)	0.05 (0.15)		9.15
CaO	2.68 (0.40)	12.60 (4.60)	0.53	23.18 (0.83)	2.81 (0.24)	12.77		22.05	3.29 (0.76)	13.95 (3.02)		22.16
Na_2O	4.15 (0.57)	3.55 (2.06)	1.60	0.13 (0.09)	4.05 (0.36)	3.69		0.31	3.65 (1.09)	2.72 (1.26)		0.39
K_2O	8.23 (0.33)	0.66 (0.52)	13.95	0.02 (0.05)	8.40 (0.70)	0.66		0.08	8.78 (1.07)	0.58 (0.64)		0.00
P_2O_5	0.11 (0.18)	0.08 (0.28)	0.19	0.01 (0.04)	0.06 (0.16)	0.00		0.18	0.13 (0.22)	0.03 (0.10)		0.26
Cl	0.69 (0.08)				0.67 (0.24)				0.52 (0.33)			
Total	97.00 (2.80)	100.44 (2.80)	100.93	99.32 (4.86)	97.82 (2.35)	100.08		100.05	98.61 (3.42)	99.80 (0.68)		99.71
$^{87}Sr/^{86}Sr$	0.707527 ± 6		0.707499 ± 6	0.707500 ± 6	0.707530 ± 7				0.707539 ± 6		0.707550 ± 6	0.707477 ± 6
$^{143}Nd/^{144}Nd$	0.512439 ± 7		-	0.512437 ± 7	0.512447 ± 7				0.512432 ± 6		0.512440 ± 6	0.512444 ± 6
Sample	**N170**				**N200**				**S1**			
phase	*glass*	*pl*	*sn*	*cpx*	*glass*	*pl*	*sn*	*cpx*	*glass*	*pl*	*sn*	*cpx*
# of analyses	12	4	0	0	10	1	0	2	11	5	1	6
SiO_2	59.55 (3.13)	50.91 (2.49)			57.21 (1.77)	47.82		44.10 (1.42)	55.82 (1.93)	52.61 (3.56)	58.74	44.58 (2.18)
TiO2	0.43 (0.35)	0.08 (0.23)			0.40 (0.39)	0.30		1.61 (1.32)	0.65 (0.53)	0.19 (0.32)	0.88	1.68 (0.85)
Al_2O_3	18.35 (1.13)	30.31 (2.51)			18.78 (0.82)	33.13		8.82 (2.92)	17.46 (2.57)	27.94 (2.33)	21.66	9.55 (2.04)
FeO	3.39 (0.80)	0.53 (0.32)			5.01 (0.83)	1.04		11.97 (2.54)	7.27 (1.91)	1.11 (0.45)	0.78	11.29 (0.86)
MnO	0.22 (0.41)	0.01 (0.03)			0.16 (0.38)	0.25		0.23 (0.00)	0.25 (0.33)	0.10 (0.28)	0.27	0.27 (0.41)
MgO	0.44 (0.19)	0.06 (0.26)			0.83 (0.28)	0.00		9.60 (0.09)	1.23 (0.31)	0.28 (0.26)	0.00	9.98 (1.03)
CaO	3.81 (1.09)	13.14 (1.39)			4.45 (1.07)	15.97		22.68 (0.33)	4.22 (2.43)	12.02 (2.25)	1.12	21.57 (1.13)
Na_2O	3.83 (0.69)	3.08 (0.65)			3.46 (0.50)	1.93		0.12 (0.12)	3.22 (0.56)	3.05 (0.74)	3.71	0.01 (0.04)
K_2O	8.62 (0.93)	0.50 (0.25)			7.88 (0.77)	0.42		0.22 (0.21)	7.21 (1.83)	1.77 (1.09)	7.49	0.30 (0.47)
P_2O_5	0.15 (0.20)	0.05 (0.21)			0.35 (0.21)	0.00		0.31 (0.21)	0.47 (0.41)	0.16 (0.36)	0.00	0.56 (0.51)
Cl	0.57 (0.15)				0.59 (0.16)				0.76 (0.31)			
Total	99.35 (4.91)	98.69 (2.12)			99.12 (2.01)	100.86		99.67 (0.58)	98.54 (2.60)	99.24 (0.99)	94.64	99.79 (2.51)
$^{87}Sr/^{86}Sr$	0.707556 ± 8		0.707506 ± 6	0.707470 ± 6	0.707602 ± 6				0.707605 ± 7		0.707534 ± 6	-
$^{143}Nd/^{144}Nd$	0.512435 ± 6		0.512429 ± 7	0.512452 ± 6	0.512436 ± 6				0.512431 ± 6		-	0.512452 ± 7

4.3. Mineral chemistry

The anorthite (An) content of plagioclase phenocrysts varies from An_{51} to An_{80} with an average increase from trachytic to latitic samples, instead in microlites of latitic scoriae (S1 sample) takes values of An_{51-77}. The sanidine shows a decrease in Or content (from Or_{84} to Or_{54}) from trachytic to latitic composition (Fig. 5a and Table 1). Ternary end-member composition plot of clinopyroxene indicates a moderate Fe enrichment with differentiation, with ferrosilite values ranging from to Fs_{38} to Fs_{45} (Fig. 5b and Table 1).

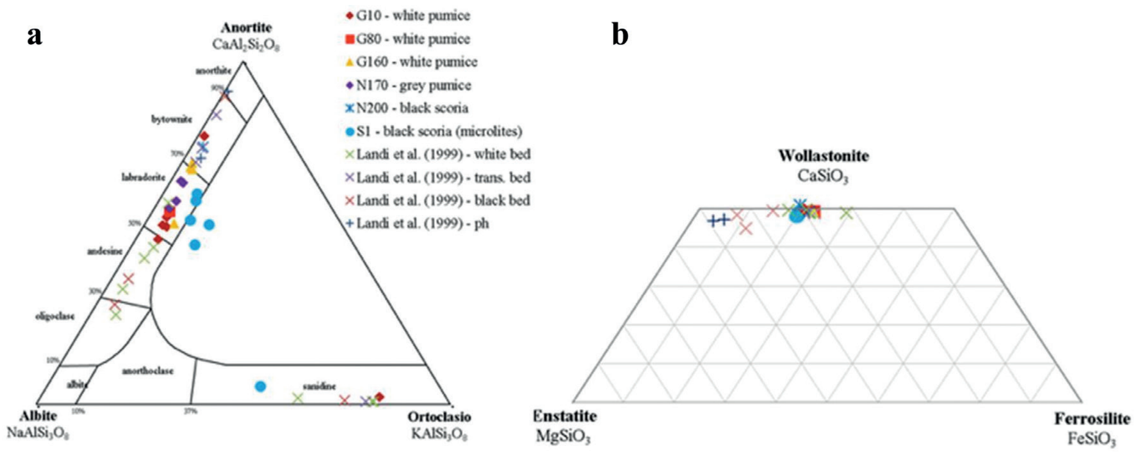

Fig. 5 - Ab-An-Or ternary (a) and Di-Hd-En-Fs quadrilater (b) diagrams showing the composition of feldspars and clinopyroxene crystals for Pomici di Base rocks. Ph = Phreatomagmatic phase. The compositional trend towards the centre of the ternary diagram for microlites in sample S1 can be the result of water exolution and the consequent increment of magma liquidus temperature during its ascent, able to promote an extensive crystallisation.

4.4. Sr and Nd isotopic composition

Sr isotopic composition varies in the analysed groundmasses from 0.707527 to 0.707605 towards the less differentiated terms. Crystal phases have $^{87}Sr/^{86}Sr$ values ranging from 0.707470-0.707500 in clinopyroxene and 0.707499-0.707500 in sanidine, which partially overlap with isotopic values of trachytic groundmasses. Nd isotopic compositions are much less variable and cluster around 0.512429-0.512452 both in matrix-glasses and minerals (Fig. 6 and Table 1).

4.5. Vesicularity and textural data

Clast vesicularity as well as density are strongly related to stratigraphic height, varying significantly during the eruption. Particularly white and intermediate pumices have a modal vesicularity of 75-76% (modal density: 0.57-0.61 g/cm^3) that increases at 48-59% (1.11-1.40 g/cm^3) in the upper black scoriae (Table 2).

Low-density pumices are characterised by at least two vesicle populations: small (< 20 μm) spherical bubbles and irregularly shaped large bubbles (> 20 μm), showing many stages of coalescence, separated by thin (few μm) microlite-free glass. Sometimes, evidence of stretched bubbles is present particularly in gray pumices. Black and high-density scoriae have

Table 2 - Key petrological features of the analysed samples.

Sample	Melt composition	Bulk vesicularity (%)	Microlite content (vol.%)
G10	Trachyte	75	-
G80	Trachyte	76	-
G160	Trachyte	76	-
N170	Trachyte	75	-
N200	Latite	59	15
S1	Latite	48	31

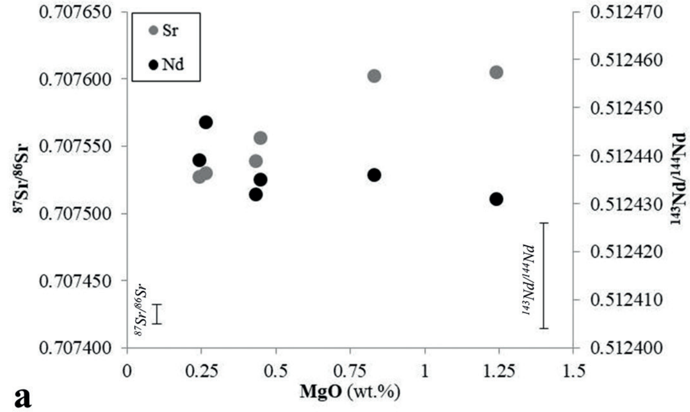

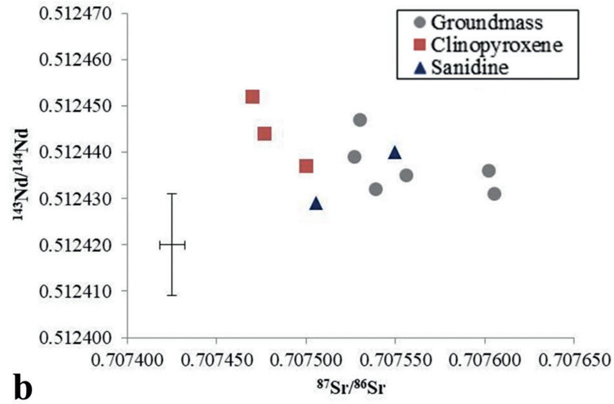

Fig. 6 - a) MgO (wt.%) vs. Sr and Nd isotopic ratios for separated groundmasses; b) $^{143}Nd/^{144}Nd$ versus $^{87}Sr/^{86}Sr$ compositions for separated groundmasses and minerals.

markedly different textures, which are characterised predominantly by small bubble population and subordinately by large polylobate, amoeboid bubbles separated by thick (> 10 μm) microlite-bearing glass (15-31 vol.%; Figs. 3 and 7, and Table 2).

Vesicle Size Distributions (VSDs, fractions for different equivalent sphere diameters) reveal polymodal trends for both white and gray pumices showing two peaks at 5-10 μm and 20-30 μm; on the contrary VSDs for black scoriae generally show a less evident bimodality with distributions skewed towards finer sizes, while larger vesicle mode is relatively poorly represented (Fig. 7).

5. Discussion

5.1. Pre-eruptive processes

Our geochemical data show the existence of a chemically-zoned magma chamber, from trachyte to latite. We have estimated pre-eruptive temperature and pressure by using the clinopyroxene-liquid thermo-barometer developed for alkaline differentiated magmas by Masotta *et al*. (2013). Particularly, thermometric calculations indicate that crystallisation temperature continuously

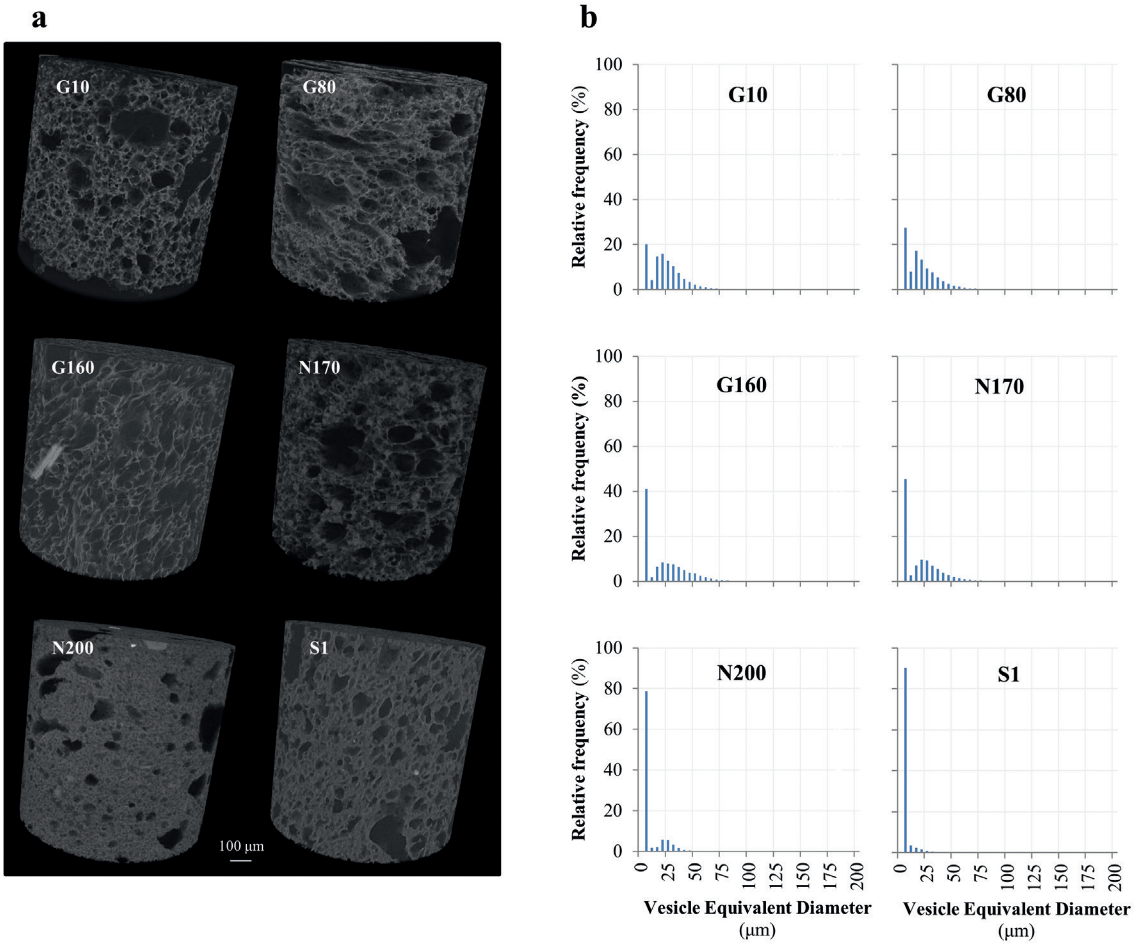

Fig. 7 - a) µCT 3D images. Volume range: 0.36-0.49 mm^3. b) Vesicle size distributions. Histograms show vesicle size frequency for Pomici di Base rocks.

increases from 907±46 °C in the upper trachytic layer to 1059±46 °C towards the basal latite with an estimated average pressure of 137±85 MPa. The last value is in agreement with the results obtained by using Cl-content on matrix-glasses (Balcone-Boissard *et al.*, 2015). In fact, an average pressure of 106±11 MPa [using Cl solubility from Signorelli and Carrol (2002) and considering an analytical uncertainty of 10% for Cl concentration] can be inferred for the upper trachytic magma. We neglected the latitic terms from this calculation due to the lack of data on Cl solubility for this melt composition and their high-microlite content that weaken the estimate. Therefore, a depth of 4.33±0.45 km can be calculated for magma chamber top assuming a lithostatic system with an average crustal density of 2.5 g/cm^3. Interestingly the two different barometers used in this work estimate similar values of storage pressures and allow to achieve useful information to better reconstruct the time evolution of the Somma-Vesuvius plumbing system, for which very few data exist on its initial eruptive periods (see Scaillet *et al.*, 2008; Balcone-Boissard *et al.*, 2015). In particular, a broad pressure range of 300-500 MPa has been further reported by Landi *et al.* (1999) for Pomici di Base compositions on the basis of two feldspars (Stormer, 1975) and feldspar-liquid (Kudo and Weill, 1970) barometers calibrated on limited databases.

Moreover, our geochemical and temperature trends suggest that factional crystallisation played a dominant role in the magma evolution from latitic to trachytic compositions. In fact, the general increase in SiO_2, Na_2O, K_2O and decrease in TiO_2, FeO, CaO, P_2O_5, together with the almost constant trend of Al_2O_3, are compatible with the crystallisation of sanidine, plagioclase, and clinopyroxene, which coherently show an average decrease in Or content, an enrichment in An content, and a reduction in Fe content respectively. However, the low crystal content in juvenile products is in contrast with the high crystallisation indicated by mass balance calculations to obtain this differentiation. These features suggest that magma was likely extracted by a crystal mush (see also Landi *et al.*, 1999).

The highest $^{87}Sr/^{86}Sr$ ratios observed in separated groundmasses respect to sanidine and clinopyroxene crystals imply the involvement of crustal contamination processes. Particularly, isotopic variations suggest that assimilation was a later process occurred mainly after precipitation of minerals. The potential influence of contamination in the petrogenesis of the analysed Pomici di Base rocks was tested using the EC-AFC (Energy-Constrained Assimilation and Fractional Crystallisation) model by Pappalardo *et al.* (2018). Best fit was obtained considering a magma contamination by limestone rocks [Triassic limestone with $^{87}Sr/^{86}Sr = 0.709$ and $^{143}Nd/^{144}Nd = 0.512$; e.g. Piochi *et al.* (2006) and Di Renzo *et al.* (2007)] at an ambient temperature of 300 °C [see De Lorenzo *et al.* (2006), for the constrained depth]. The results show that the observed Sr and Nd isotopic variation is justified by the ingestion of 2-4% of carbonate rocks by a magma, which has crystallised for about 55% of its initial mass. The carbonatic contamination hypothesis is also supported by the abundance of carbonatic metamorphosed clasts found in the Pomici di Base deposits and juvenile rocks (Bertagnini *et al.*, 1998; Landi *et al.*, 1999). Experimental data show that the contamination by carbonate country rocks [extended from about 2 to 10 km beneath Somma-Vesuvius; e.g. Berrino *et al.* (1998)] during magma storage promotes the release of large amounts of CO_2-rich fluids and consequently can be cause of ignition and/or increase of the degree of explosiveness of the eruption (e.g. Iacono Marziano *et al.*, 2008; Deegan *et al.*, 2010, 2011; Mollo *et al.*, 2010; Jolis *et al.*, 2013; Blythe *et al.*, 2015). However, the high values of Sr isotopic ratios in latitic groundmasses, in disequilibrium with phenocrysts and trachytic glasses, indicate more complex contamination mechanisms (see below).

5.2. Syn-eruptive processes

White and gray trachytic pumices, erupted from a stable plume during an early stage of the Plinian phase, show polymodal VSDs trends suggesting different nucleation stages. Particularly, the large vesicles population represents the early-formed bubbles with varying history of interaction and coalescence, while the population of small bubbles reflects a late-stage nucleation event in the shallow conduit and then depicts the vesiculation state of the magma at the time of fragmentation (Baker *et al.*, 2012; Gonnermann and Houghton, 2012; Liedl *et al.*, 2019). The evidence of coalescence between larger bubbles, separated by thin films of matrix-glass (1 to 10 μm), associated to high degree of vesiculation suggest that bubble growth has occurred up to the achievement of a porosity threshold [65-75%; e.g. Sparks (1978); Gardner *et al.* (1996)], at which the experimental data indicate an abrupt increase in permeability with a small increment in vesicularity (Takeuchi *et al.*, 2009; Rust and Cashman, 2011). These data suggest that fragmentation is most likely to occur under closed-system degassing conditions when the magma exceeds the critical porosity (between 70-80%). In particular, in case of rapid magma ascent in volcanic conduit, the gas fails to move away from the liquid even when it is characterised from a high permeability, thus favouring the expansion of the gas that leads to the fragmentation. Rapid ascent rate is confirmed by the absence of microlites in the pumice samples, in agreement with decompression experiments showing non-crystallisation of microlites in the case of ascent rates lower than few hours [e.g. a delay of ~1-4 hours in the nucleation of microlites after decompression has been observed by Couch *et al*. (2003)].

Latitic black-scoriae, erupted at the end of this sustained-column phase, show lower porosity associated to the presence of polylobate thick-walled bubbles and microlite-bearing groundmass glass. These features suggest that the more mafic and less viscous melt, about the 75% of the total involved magma during this eruption (Landi *et al*., 1999), suffered at shallow level, during rising from a deep source, outgassing and decompression-induced microlite growth, producing abrupt rheological changes. In this scenario the dominant presence of small round bubbles represent a late stage vesiculation of the partially degassed magma, that has been, in this way, forced to erupt explosively. New available textural data (Pappalardo *et al*., 2018) suggest that this nucleation event was triggered by the ongoing decarbonation process and the related conspicuous release of CO_2-rich fluids that was more intense in these hot less-evolved liquids. This hypothesis is supported by the high Sr isotopic ratios in latitic groundmass. High temperature and pressure carbonate assimilation experiments demonstrated that decarbonation can be very fast [minutes to days; e.g. Deegan *et al*. (2011) and Blythe *et al*. (2015)] and may promote the migration of CO_2 bubbles from the dissolving carbonate throughout the magma so enhancing the ability of the magma itself to erupt explosively (Freda *et al*., 2010; Dallai *et al*., 2011).

6. Conclusions

Here we present our preliminary results of a geochemical, isotopic and textural study performed on pyroclasts emitted during the caldera-forming Pomici di Base (22 ka) Plinian eruption from Somma-Vesuvius volcano.

Particularly geochemical and isotopic data suggest the existence, immediately before the eruption, of a magma chamber with a top located at a depth of about 4.5 km and characterised by a compositional (from trachyte to latite) and thermal (from ~900 to 1050 °C) zoning. Magmas, geochemically cogenetic, were probably extracted from a crystal-rich mush zone in the magma reservoir. However, the variation of Sr and Nd isotopic ratios indicates the occurrence of a crustal (limestone) contamination process (< 5%), and a subsequent CO_2 liberation, during magma storage.

Textural data suggest a degassing process under closed-system conditions at the beginning of the Plinian fallout phase, during the fast emission of trachitic magmas. In contrast, during the following emission of latitic magmas, the degassing took place under open-system conditions, at decreasing decompression rates thus producing the collapse of the eruptive column and the consequent triggering of the phreatomagmatic phase.

Acknowledgements. The results of this paper were presented at the 36th National Congress GNGTS, 14-16 November 2017, Trieste, Italy. The authors wish to thank I. Arienzo (INGV-OV), R. de Gennaro (University of Naples Federico II) for essential helps during isotopic and SEM-EDS analyses, respectively. We acknowledge two anonymous reviewers for suggestions that greatly improved the manuscript.

REFERENCES

Andronico D., Calderoni G., Cioni R., Sbrana A., Sulpizio R. and Santacroce R.; 1995: *Geological map of Somma-Vesuvius volcano*. Per. Mineral., **64**, 77-78.

Ayuso R.A., De Vivo B., Rolandi G., Seal II R.R. and Paone A.; 1998: *Geochemical and isotopic (NdPb-Sr-O) variations bearing on the genesis of volcanic rocks from Vesuvius, Italy*. J. Volcanol. Geotherm. Res., **82**, 53-78.

Baker D.R., Mancini L., Polacci M., Higgins M.D., Gualda G.A.R., Hill R.J. and Rivers M.L.; 2012: *An introduction to the application of X-ray microtomography to the three-dimensional study of igneous rocks*. Lithos, **148**, 262-276.

Balcone-Boissard H., Boudon G., Cioni R., Webster J.D., Zdanowicz G., Orsi G. and Civetta L.; 2015: *Chlorine as a geobarometer for alkaline magmas: evidence from a systematic study of the eruptions of Mount Somma - Vesuvius*. Sci. Rep., **6**, 21726.

Belkin H.E. and De Vivo B.; 1993: *Fluid inclusion studies of ejected nodules from Plinian eruptions of Mt. Somma-Vesuvius*. J. Volcanol. Geotherm. Res., **58**, 98-100.

Berrino G., Corrado G. and Riccardi U.; 1998: *Sea gravity data in the Gulf of Naples: a contribution to delineating the structural pattern of the Vesuvian area*. J. Volcanol. Geotherm. Res., **82**, 139-150.

Bertagnini A., Landi P., Rosi M. and Vigliargio A.; 1998: *The Pomici di Base plinian eruption of Somma-Vesuvius*. J. Volcanol. Geotherm. Res., **83**, 219-239.

Blundy J. and Cashman K.; 2008: *Petrologic reconstruction of magmatic system variables and processes*. Rev. Mineral. Geochem., **69**, 179-239.

Blythe L.S., Deegan F.M., Freda C., Jolis E.M., Masotta M., Misiti V., Taddeucci J. and Troll V.R.; 2015: *CO_2 bubble generation and migration during magma-carbonate interaction*. Contrib. Mineral. Petrol., **169**, 1-16.

Borgia A., Tizzani P., Solaro G., Manzo M., Casu F., Luongo G., Pepe A., Berardino P., Fornaro G., Sansosti E., Ricciardi G.P., Fusi N., Di Donna G. and Lanari R.; 2005: *Volcanic spreading of Vesuvius, a new paradigm for interpreting its volcanic activity*. Geophys. Res. Lett., **32**, L03303.

Capaldi G., Gillot P.Y., Munno R., Orsi G. and Rolandi G.; 1985: *Sarno Formation: the major plinian eruption of the Somma-Vesuvius*. In: Abstracts, Scientific Assembly, IAVCEI 1985, Giardini di Naxos, Italy.

Cioni R.; 2000: *Volatile content and degassing processes in the AD 79 magma chamber at Vesuvius (Italy)*. Contrib. Mineral. Petrol., **140**, 40-54.

Cioni R., Marianelli P. and Santacroce R.; 1998: *Thermal and compositional evolution of the shallow magma chambers of Vesuvius: evidence from pyroxene phenocrysts and melt inclusions*. J. Geophys. Res., **103**, 18277-18294.

Cioni R., Santacroce R. and Sbrana A.; 1999: *Pyroclastic deposits as a guide for reconstructing the multi-stage evolution of the Somma-Vesuvius Caldera*. Bull. Volcanol., **60**, 207-222.

Cioni R., Bertagnini A., Santacroce R. and Andronico D.; 2008: *Explosive activity and eruption scenarios at Somma-Vesuvius (Italy): towards a new classification scheme*. J. Volcanol. Geotherm. Res., **178**, 331-346.

Cioni R., Bertagnini A., Andronico D., Cole P.D. and Mundula F.; 2011: *The 512 AD eruption of Vesuvius: complex dynamics of a small scale subplinian event*. Bull. Volcanol., **73**, 789-810.

Civetta L., Galati R. and Santacroce R.; 1991: *Magma mixing and convective compositional layering within the Vesuvius magma chamber*. Bull. Volcanol., **53**, 287-300.

Cnudde V. and Boone M.N.; 2013: *High-resolution X-ray computed tomography in geosciences: a review of the current technology and applications*. Earth Sci. Rev., **123**, 1-17.

Cole P.D. and Scarpati C.; 2010: *The 1944 eruption of Vesuvius, Italy: combining contemporary accounts and field studies for a new volcanological reconstruction*. Geol. Mag., **147**, 391-415.

Couch S., Sparks R.S.J. and Carroll M.R.; 2003: *The kinetics of degassing-induced crystallization at Soufriere Hills volcano, Montserrat*. J. Petrol., **44**, 1477-1502.

Cubellis E., Marturano A. and Pappalardo L.; 2016: *The last Vesuvius eruption in March 1944: reconstruction of the eruptive dynamic and its impact on the environment and people through witness reports and volcanological evidence*. Nat. Hazards, **82**, 95-121, doi: 10.1007/s11069-016-2182-7.

Dallai L., Cioni R., Boschi C. and D'Oriano C.; 2011: *Carbonate-derived CO_2 purging magma at depth: influence on the eruptive activity of Somma-Vesuvius, Italy*. Earth Planet. Sci. Lett., **310**, 84-95.

De Lorenzo S., Di Renzo V., Civetta L., D'Antonio M. and Gasparini P.; 2006: *Thermal model of the Vesuvius magma chamber*. Geophys. Res. Lett., **33**, L17302.

De Vivo B., Petrosino P., Lima A., Rolandi G. and Belkin H.E.; 2010: *Research progress in volcanology in the Neapolitan area, southern Italy: a review and some alternative views*. Mineral. Petrol., **99**, 1-28.

Deegan F.M., Troll V.R., Freda C., Misiti V., Chadwick J.P., McLeod C.L. and Davidson J.P.; 2010: *Magma-carbonate interaction processes and associated CO_2 release at Merapi Volcano, Indonesia: insights from experimental petrology*. J. Petrol., **51**, 1027-1051.

Deegan F.M., Troll V.R., Freda C., Misiti V. and Chadwick J.P.; 2011: *Fast and furious: crustal CO_2 release at Merapi volcano, Indonesia*. Geol. Today, **27**, 57-58.

Del Moro A., Fulignati P., Marianelli P. and Sbrana A.; 2001: *Magma contamination by direct wall rock interaction: constraints from xenoliths from the wall of carbonate-hosted magma chamber (Vesuvius 1944 eruption)*. J. Volcanol. Geotherm. Res., **112**, 15-24, doi: 10.1016/S0377-0273(01)00231-1.

Delibrias G., Di Paola G.M., Rosi M. and Santacroce R.; 1979: *La storia eruttiva del complesso vulcanico Somma-Vesuvio ricostruita dalle successioni piroclastiche del Monte Somma*. Rend. Soc. Ital. Mineral. Petrol., **35**, 411-438.

Di Renzo V., Di Vito M.A., Arienzo I., Carandente A., Civetta L., D'Antonio M., Giordano F., Orsi G. and Tonarini S.; 2007: *Magmatic history of Somma-Vesuvius on the basis of new geochemical and isotopic data from a deep borehole (Camaldoli della Torre)*. J. Petrol., **48**, 753-784.

Freda C., Gaeta M., Giaccio B., Marra F., Palladino D.M., Scarlato P. and Sottili G.; 2010: *CO_2- driven large mafic explosive eruptions: the Pozzolane Rosse case study from the Colli Albani Volcanic District (Italy)*. Bull. Volcanol., **73**, 241-256, doi: 10.1007/s00445-010-0406-3.

Fulignati P., Gioncada A. and Sbrana A.; 1995: *The magma chamber related hydrothermal system of Vesuvius, first mineralogical and fluid inclusion data on hydrothermalized subvolcanic and lavic samples from phreatomagmatic eruptions*. Per. Mineral., **64**, 185-187.

Fulignati P., Marianelli P. and Sbrana A.; 1998: *New insights on the thermometamorphic-metasomatic magma chamber shell of the 1944 eruption of Vesuvius*. Acta Vulcanol., **10**, 47-54.

Gardner J.E., Thomas R.M.E., Jaupart C. and Tait S.; 1996: *Fragmentation of magma during Plinian volcanic eruptions*. Bull. Volcanol., **58**, 144-162.

Gilg H.A., Lima A., Somma R., Ayuso R.A., Belkin H.E. and De Vivo B.; 1999: *A fluid inclusion and isotope study of calc-silicate ejecta from Mt. Somma-Vesuvius: evidence for interaction of high-temperature hypersaline fluids with the sedimentary basement*. Terra Nostra, **99**, 118-120.

Gilg H.A., Lima A., Somma R., Belkin H.E., De Vivo B. and Ayuso R.A.; 2001: *Isotope geochemistry and fluid inclusions study of skarns from Vesuvius*. Mineral. Petrol., **73**, 145-176.

Gonnermann H.M. and Manga M.; 2007: *The fluid mechanics inside a volcano*. Annu. Rev. Fluid Mech., **39**, 321-356.

Gonnermann H.M. and Houghton B.F.; 2012: *Magma degassing during the Plinian eruption of Novarupta, Alaska, 1912*. Geochem. Geophys. Geosyst., **13**, Q10009.

Houghton B.F. and Wilson C.J.N.; 1989: *A vesicularity index for pyroclastic deposits*. Bull. Volcanol., **51**, 451-462.

Houghton B.F., Carey R.J., Cashman K.V., Wilson C.J.N., Hobdenm B.J. and Hammer J.E.; 2010: *Diverse patterns of ascent, degassing, and eruption of rhyolite magma during the 1.8 ka Taupo eruption, New Zealand: evidence from clast vesicularity*. J. Volcanol. Geotherm. Res., **195**, 31-47.

Iacono Marziano G., Gaillard F. and Pichavant M.; 2008: *Limestone assimilation by basaltic magmas: an experimental re-assessment and application to Italian volcanoes*. Contrib. Mineral. Petrol., **155**, 719-738.

Iacono Marziano G., Gaillard F., Scaillet B., Pichavant M. and Chiodini G.; 2009: *Role of non-mantle CO_2 in the dynamics of volcano degassing: the Mount Vesuvius example*. Geol., **37**, 319-322.

Jolis E.M., Freda C., Troll V.R., Deegan F.M., Blythe L.S., McLeod C.L. and Davidson J.P.; 2013: *Experimental simulation of magma-carbonate interaction beneath Mt. Vesuvius, Italy*. Contrib. Mineral. Petrol., **166**, 1335-1353.

Jolis E.M., Troll V.R., Harris C., Freda C., Gaeta M., Orsi G. and Siebe C.; 2015: *Skarn xenolith record crustal CO_2 liberation during Pompeii and Pollena eruptions, Vesuvius volcanic system, central Italy*. Chem. Geol., **415**, 17-36.

Joron J.L., Metrich N., Rosi M., Santacroce R. and Sbrana A.; 1987: *Chemistry and petrography*. Quaderni La Ricerca Scientifica, **114**, 105-174.

Kudo A.M. and Weill D.F.; 1970: *An igneous plagioclase thermometer*. Contrib. Mineral. Petrol., **25**, 62-65.

Landi P., Bertagnini A. and Rosi M.; 1999: *Chemical zoning and crystallization mechanisms in the magma chamber of the Pomici di Base Plinian eruption of Somma-Vesuvius (Italy)*. Contrib. Mineral. Petrol., **135**, 179-197.

Liedl A., Buono G., Lanzafame G., Dabagov S.B., Della Ventura G., Hampai D., Mancini L., Marcelli A. and Pappalardo L.; 2019: *A 3D imaging textural characterization of pyroclastic products from the 1538 CE Monte Nuovo eruption (Campi Flegrei, Italy)*. Lithos, **340-341**, 316-331, doi: 10.1016/j.lithos.2019.05.010.

Lima A., Danyushevsky L.V., De Vivo B. and Fedele L.; 2003: *A model for the evolution of the Mt. Somma-Vesuvius magmatic system based on fluid and melt inclusion investigations*. In: De Vivo B. and Bodnar R.J. (eds), Melt inclusions in volcanic systems: methods, applications and problems, Elsevier, New York, NY, USA, pp. 227-249.

Marianelli P., Métrich N., Santacroce R. and Sbrana A.; 1995: *Mafic magma batches at Vesuvius: a glass inclusion approach to the modalities of feeding stratovolcanoes*. Contrib. Mineral. Petrol., **120**, 159-169.

Marianelli P., Metrich N. and Sbrana A.; 1999: *Shallow and deep reservoirs involved in magma supply of the 1944 eruption of Vesuvius*. Bull. Volcanol., **61**, 48-63.

Marianelli P., Sbrana A., Metrich N. and Cechetti A.; 2005: *The deep feeding system of Vesuvius involved in recent violent Strombolian eruptions*. Geophys. Res. Lett., **32**, L2306.

Masotta M., Mollo S., Freda C., Gaeta M. and Moore G.; 2013: *Clinopyroxene-liquid thermometers and barometers specific to alkaline differentiated magmas*. Contrib. Mineral. Petrol., **166**, 1545-1561.

Mastrolorenzo G. and Pappalardo L.; 2006: *Magma degassing and crystallization processes during eruptions of high-risk Neapolitan volcanoes: evidence of common equilibrium rising processes in alkaline magmas*. Earth Planet. Sci. Lett., **250**, 164-181.

Mollo S., Gaeta M., Freda C., Di Rocco T., Misiti V. and Scarlato V.; 2010: *Carbonate assimilation in magmas: a reappraisal based on experimental petrology*. Lithos, **114**, 503-514.

Morabito S., Petrosino P., Milia A., Sprovieri M. and Tamburrino S.; 2014: *A multidisciplinary approach for reconstructing the stratigraphic framework of the last 40 ka in a bathial area of the eastern Tyrrhenian Sea*. Global Planet. Change, **123**, 121-138, doi: 10.1016/j.gloplacha.2014.10.005.

Pappalardo L. and Mastrolorenzo G.; 2010: *Short residence times for alkaline Vesuvius magmas in a multi-depth supply system: evidence from geochemical and textural studies*. Earth Planet. Sci. Lett., **296**, 133-143.

Pappalardo L. and Mastrolorenzo G.; 2012: *Rapid differentiation in sill-like magma reservoir: a case study from the Campi Flegrei Caldera*. Sci. Rep., **2**, 712, doi: 10.1038/srep00712.

Pappalardo L., Piochi M. and Mastrolorenzo G.; 2004: *The 35500 yr BP-1944 AD magma plumbing system of Somma-Vesuvius: constraints on its behaviour and present state through a review of isotope data*. Ann. Geophys., **47**, 1363-1375.

Pappalardo L., D'Auria L., Cavallo A. and Fiore S.; 2014: *Petrological and seismic precursors of the paroxysmal phase of the last Vesuvius eruption on March 1944*. Sci. Rep., **4**, 6297, doi: 10.1038/srep06297.

Pappalardo L., Buono G., Fanara S. and Petrosino P.; 2018: *Combining textural and geochemical investigations to explore the dynamics of magma ascent during Plinian eruptions: a Somma-Vesuvius volcano (Italy) case study*. Contrib. Mineral. Petrol., **173**, 61, doi: 10.1007/s00410-018-1486-x.

Peccerillo A.; 2005: *Plio-Quaternary volcanism in Italy*. Springer, Berlin, Germany, 365 pp.

Pichavant M., Scaillet B., Pommier A., Iacono-Marziano G. and Cioni R.; 2014: *Nature and evolution of primitive Vesuvius magmas: an experimental study*. J. Petrol., **55**, 2281-2310.

Piochi M., Ayuso R.A., De Vivo B. and Somma R.; 2006: *Crustal contamination and crystal entrapment during polybaric magma evolution at Mt. Somma-Vesuvius volcano, Italy: geochemical and Sr isotope evidence*. Lithos, **86**, 303-329.

Rust A.C. and Cashman K.V.; 2011: *Permeability controls on expansion and size distributions of pyroclasts*. J. Geophys. Res., **116**, B11202.

Santacroce R.; 1987: *Somma-Vesuvius*. Quaderni La Ricerca Scientifica, **114**, 1-251.

Santacroce R., Bertagnini A., Civetta L., Landi P. and Sbrana A.; 1993: *Eruptive dynamics and petrogenetic processes in a very shallow magma reservoir: the 1906 eruption of Vesuvius*. J. Petrol., **34**, 383-425.

Santacroce R., Cioni R., Marianelli P., Sbrana A., Sulpizio R., Zanchetta G., Donahue D.J. and Joron J.L.; 2008: *Age and whole rock-glass compositions of proximal pyroclastics from the major explosive eruptions of Somma-Vesuvius: a review as a tool for distal tephrostratigraphy*. J. Volcanol. Geotherm. Res., **177**, 1-18.

Savelli C.; 1968: *The problem of rock assimilation by Somma-Vesuvius magmas, II. Composition of sedimentary rocks and carbonate ejecta from Vesuvius Area*. Contrib. Mineral. Petrol., **18**, 43-64.

Scaillet B., Pichavant M. and Cioni R.; 2008: *Upward migration of Vesuvius magma chamber over the past 20.000 years*. Nature, **455**, 216-219.

Scandone R., Cashman K. and Malone S.D.; 2007: *Magma supply, magma ascent and the style of volcanic eruptions*. Earth Planet. Sci. Lett., **253**, 513-529.

Shea T., Houghton B.F., Gurioli L., Cashman K.V., Hammer J.E. and Hobden B.J.; 2010: *Textural studies of vesicles in volcanic rocks: an integrated methodology*. J. Volcanol. Geotherm. Res., **190**, 271-289.

Shea T., Gurioli L., and Houghton B.F.; 2012: *Transitions between fall phases and pyroclastic density currents during the AD 79 eruption at Vesuvius: building a transient conduit model from the textural and volatile record*. Bull. Volcanol., **74**, 2363-2381.

Siani G., Sulpizio R., Paterne M. and Sbrana A.; 2004: *Tephrostratigraphy study for the last 18,000 14C years in a deep-sea sediment sequence for the South Adriatic*. Quat. Sci. Rev., **23**, 2485-2500.

Signorelli S. and Carroll M.R.; 2002: *Experimental study of Cl solubility in hydrous alkaline melts: constraints on the theoretical maximum amount of Cl in trachytic and phonolitic melts*. Contrib. Mineral. Petrol., **143**, 209-218.

Sparks R.J.S.; 1978: *The dynamics of bubble formation and growth in magmas: a review and analysis*. J. Volcanol. Geotherm. Res., **3**, 1-37.

Stormer J.C.; 1975: *A practical two-feldspar geothermometer*. Am. Mineral., **60**, 667-674.

Tait S., Thomas R., Gardner J. and Jaupart C.; 1998: *Constraints on cooling rates and permeabilities of pumice in an explosive eruption jet from colour and magnetic mineralogy*. J. Volcanol. Geotherm. Res., **86**, 79-91.

Takeuchi S., Tomiya A. and Shinohara H.; 2009: *Degassing conditions for permeable silicic magmas: implications from decompression experiments with constant rates*. Earth Planet. Sci. Lett., **283**, 101-110.

Thomas R.M.E. and Sparks R.S.J.; 1992: *Cooling of tephra during fallout from eruption columns*. Bull. Volcanol., **54**, 542-553.

Trigila R. and De Benedetti A.; 1993: *Petrogenesis of Vesuvius historical lavas constrained by Pearce element ratios analysis and experimental phase equilibria*. J. Volcanol. Geotherm. Res., **58**, 315-343.

Zdanowicz G., Boudon G., Balcone-Boissard H., Cioni R., Mundula F., Orsi G., Civetta L. and Agrinier P.; 2018: *Geochemical and textural constraints on degassing processes in sub-Plinian eruptions: case-study of the Greenish Pumice eruption of Mount Somma-Vesuvius*. Bull. Volcanol., **80**, 38, doi: 10.1007/s00445-018-1213-5.

Corresponding author: Gianmarco Buono
Istituto Nazionale di Geofisica e Vulcanologia, Osservatorio Vesuviano
Via Diocleziano 328, 80124 Napoli, Italy
Phone: +39 081 6108445; e-mail: gianmarco.buono@unina.it